Appl. Phys. A 28, 229–233 (1982)

The Dielectric Constant of PbTe at 4.2 K and $\tilde{\nu} = 84.15\,\mathrm{cm}^{-1}$, $96.97\,\mathrm{cm}^{-1}$, $103.60\,\mathrm{cm}^{-1}$

M. Tacke and W. Schuberth*
Physikalisches Institut, Universität, D-8700 Würzburg, Fed. Rep. Germany

C. R. Becker and L. D. Haas
AEG-Telefunken Serienprodukte AG, D-7100 Heilbronn, Fed. Rep. Germany

Received 8 March 1982/Accepted 20 April 1982

Abstract. The dielectric constant of a PbTe epitaxial layer has been measured by surface wave spectroscopy using an optically pumped far-infrared laser and the technique of attenuated total reflection.

PACS: 77, 42.80

It is very difficult to measure the dielectric constant ε at frequencies where its real part ε_r is negative. This is due to a large and nearly constant reflectivity, and in addition to an usually high absorption constant. However, whenever the real part ε_r is smaller than -1, surface waves may exist [1]. Their dispersion is determined by the dielectric constant. If the imaginary part of the dielectric constant, ε_i, is not too large, the surface wave dispersion may be measured quite exactly. This leads to data for the dielectric constant.

The optical constants of PbTe below the plasma frequency have usually been inferred from an oscillator fit to reflection data, e.g. [2–5]. A direct determination of the lattice contribution to the dielectric constant was made possible by a magneto-optical measurement [6] using the stripline technique [7]. In this paper, we shall describe a surface wave spectroscopy experiment for the measurement of ε in the reststrahlen region.

The Experimental Technique

A hole coupled, optically pumped FIR laser was used as a radiation source. The laser beam was collimated with a quartz lens. Excitation of the surface waves was achieved by the method of attenuated total reflection [1], using a polyethylene prism and spacers between the prism and the sample. Prism and sample were mounted in a liquid helium cryostat (Fig. 1) and could be rotated perpendicular to the optical path. Further information on the set up may be found in [8].

By scanning the angle α, the wave vector β of the electric field which penetrates into the gap below the totally internal reflecting prism base is varied, according to the equation $\beta = n_p \cdot (\omega/c) \sin\alpha$, where n_p is the refractive index of the prism, ω the frequency of light and c the speed of light in vacuum. A resonance with a surface wave on the sample shows up as a minimum of the internally reflected beam. The shape of this minimum is described by Fresnel's equation, given for example in [14].

The internal angle α has to be deduced from the external angle of incidence. Thus we have to know the prism refractive index n_p, and the refractive index n_{He} of liquid helium for the wavelengths of interest. For liquid helium we used $n_{He} = 1.0243 \pm 0.0003$, which is extrapolated from the data in the literature, where n_{He} was determined to be 1.02430 ± 0.00024 at 9.1 GHz [9] and 1.024511 ± 0.000040 at 549 THz [10]. The refractive index of the prism material polyethylene was measured by its refraction [8] to be at 4.2 K:

* Present address: Forschungsinstitut für Optik, Schloß Kreßbach, D-7400 Tübingen, Fed. Rep. Germany

0721-7250/82/0028/0229/$01.00

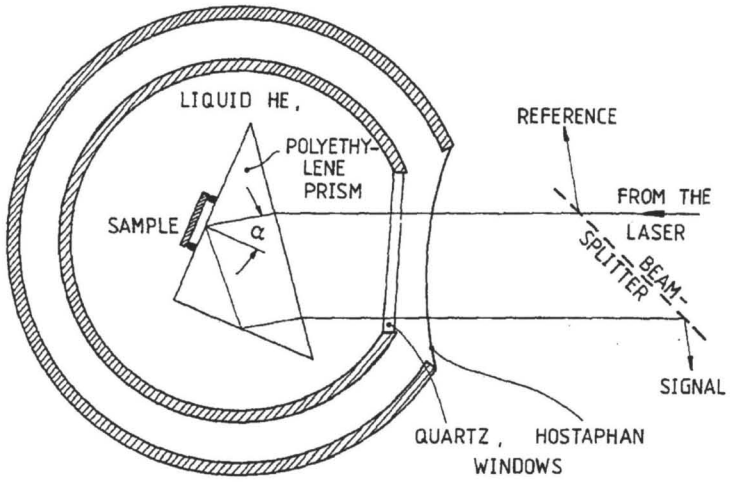

Fig. 1. The experimental set up. Hostaphan is a registered trade name, and similar to Mylar

$n_p \pm 0.005$	$\tilde{\nu}$ [cm^{-1}]
1.563	84.15
1.569	96.97
1.565	103.60

Since the sample was mounted in a cryostat, it would have been difficult to make measurements with and without a sample behind the prism, in order to determine the reflection change induced by the sample. Therefore, we measured the reflection in both the TM (p) and TE (s) polarisation of the beam and used the ratio of these values, corrected for the different reflections at the prism entrance face. The TE polarized laser beam cannot couple to the TM surface waves.

Figure 2 shows the experimental points together with a fit to Fresnel's equation. There is considerable scatter in the data due to a low signal intensity which is caused by reflection losses of the numerous reflecting dielectric surfaces. Additionally, helium bubbles in the light path seemed to contribute some noise to the signal.

The best fit was computed by minimizing the mean square deviation of the experimental data from the theoretical values. The results for ε are shown in the following table.

The stated error limits were computed by using the largest and lowest possible values for the gap width d,

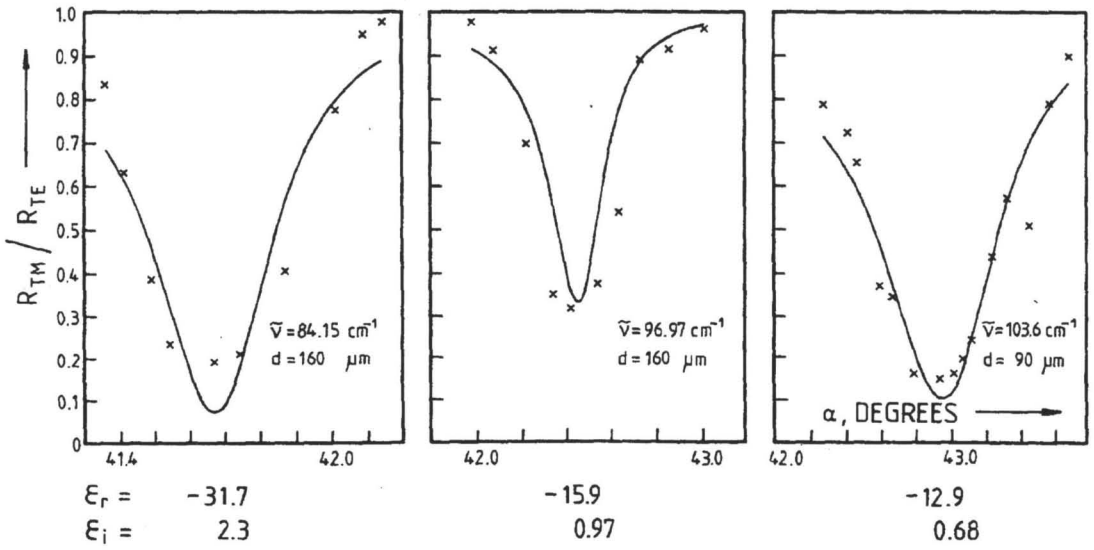

Fig. 2. The attenuated reflection versus the angle of incidence α. The experimental points are shown together with the theoretical result from Fresnel's equations. The values of ε obtained by a fit of the data to Fresnel's equation are given below the graphs, d being the width of the gap between prism and sample

Table 1. The experimental values of ε for PbTe at 4.2 K from a best fit calculation

ε_r	ε_i	$\tilde{\nu}$ [cm^{-1}]
$-(32^{+9}_{-6})$	$2.3^{+1.5}_{-0.8}$	84.15
$-(16 \pm 2)$	1 ± 0.2	96.97
$-(12.9 \pm 1.4)$	0.7 ± 0.3	103.60

which is measured to $\pm 10\,\mu$m, and the angle α to $\pm 5'$. These error limits are much larger than the statistical errors of each individual fit as computed from the program. This evaluation of ε requires, that the electromagnetic radiation be a plane wave. Even though the finite dimensions of the sample (diameter 8 mm) are still quite large compared to the wavelength of 0.1 mm, they introduce a systematic error into the preceding calculation. The beam cannot be described exactly by a single wavevector β, but rather by a distribution around β with a linewidth of the order of 1 cm^{-1}. An evaluation of ε neglecting this additional width, and its widening of the reflection minimum, overestimates systematically the imaginary part of ε.

In order to get a feeling for the influence of this effect, both the imaginary and real parts of ε were varied, such that the minimum in the curve of R_{TM}/R_{TE} versus angle α, stays at the same angular position as shown in Fig. 3. It turns out that the required value of ε_r hardly changes whereas ε_i has a larger effect. The value of R_{TM}/R_{TE} at the minimum depends strongly on ε_i. This dependence is shown in Fig. 4. Because ε_i is a function of the value of R_{TM}/R_{TE} at the minimum, we may use this value to determine ε_i. In fact, it turns out that the imaginary part of ε as determined by plane wave analysis is systematically too large, as expected. Table 2 contains the values of ε as derived by the position of the minimum and the reflectance:

Table 2

ε_r	ε_i	$\tilde{\nu}$ [cm^{-1}]
$-(32^{+4}_{-3})$	$1.6^{+0.7}_{-0.5}$	84.15
$-(16 \pm 1)$	$0.9^{+0.6}_{-0.4}$	96.97
$-(13 \pm 0.7)$	$0.6^{+0.3}_{-0.24}$	103.60

This correction procedure does not change the values of ε_r, even with a smaller assumed error due to the uncertainties in d and α, but the values of ε_i are somewhat smaller, and also have increased uncertainty limits. Thus we consider the values in Table 1 as corrected experimental values, and we note that the possible range of ε is the same as the range of ε_r in

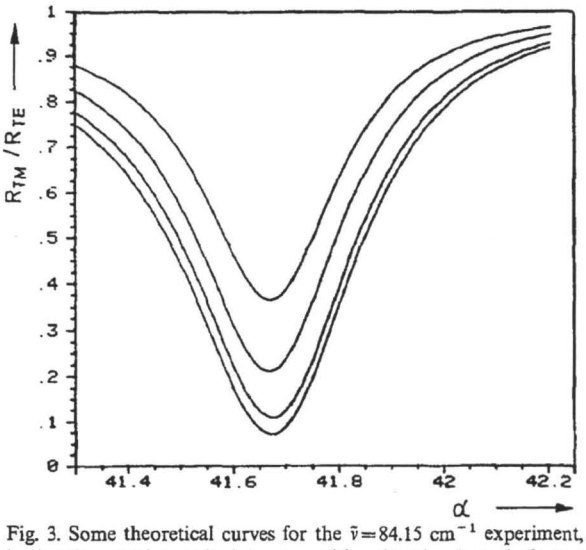

Fig. 3. Some theoretical curves for the $\tilde{\nu} = 84.15$ cm^{-1} experiment, having the experimental minimum position. Starting from the lowest curve, the ε values are: $-31.7+8.3i$, $-31.8+2i$, $-32+1.5i$, $-32+i$. The real part of ε hardly depends on the choice of the imaginary part

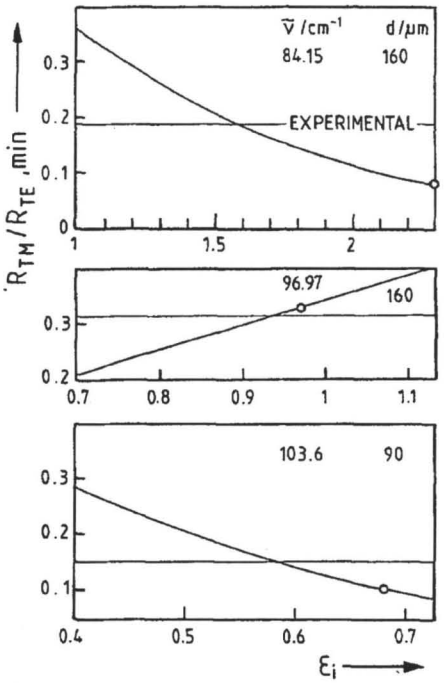

Fig. 4. Theoretical values of the minimum reflection as a function of the imaginary part of ε, computed for the experimental parameters. The values of ε_i derived by plane wave theory (open circles) systematically overestimate ε_i, as can be seen from the experimental value of the reflection. This is due to the finite size of the sample

Table 1, the upper limit of ε_i has to be taken from the first, and the lower limit from the second table.

The PbTe sample is a 40 μm thick epitaxial layer that was grown on a BaF_2 substrate by the hot wall technique with the following growth parameters:

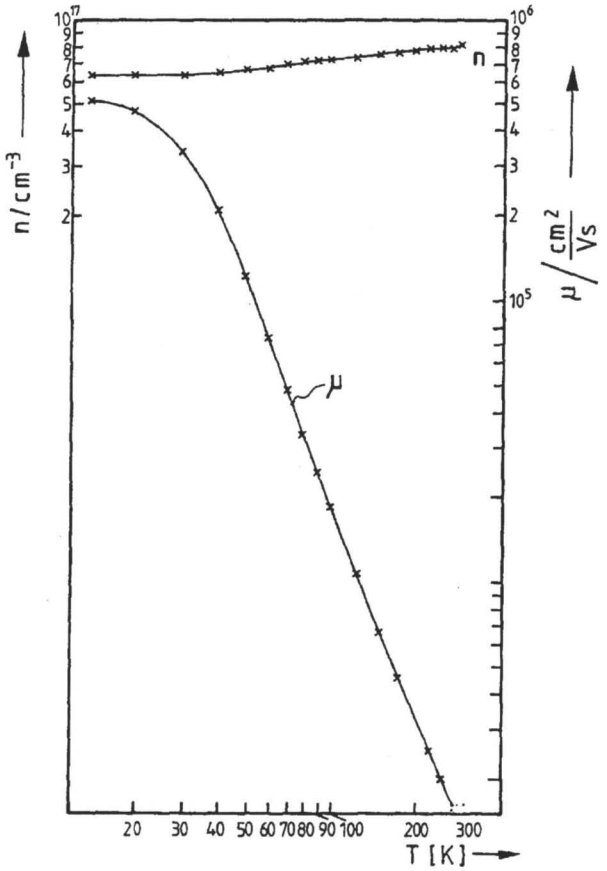

Fig. 5. Mobility and carrier concentration of the sample as a function of the temperature

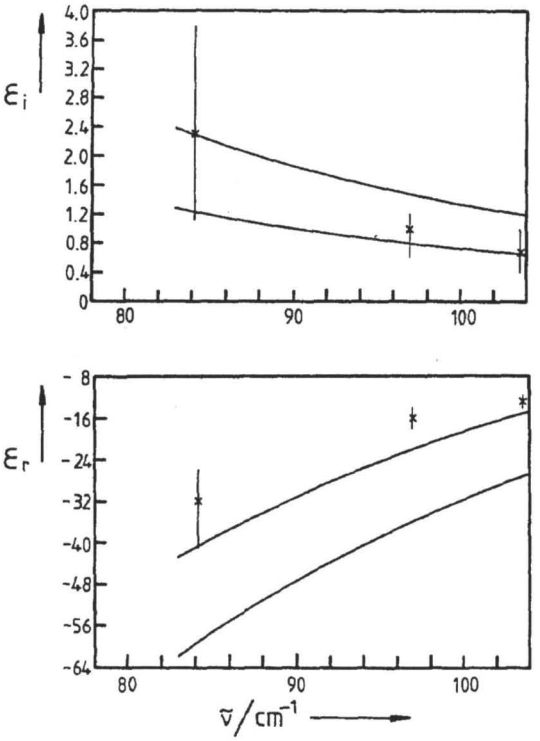

Fig. 6. The experimental values of ε_i and ε_r with their error bars are compared with the highest and lowest theoretical curves possible for the parameters taken from the literature. The electron damping parameter Γ was chosen for the best fit of the curve to the experimental values. The real part makes it obvious, that the set of parameter values (given in a table in the text) is not valid for our sample

substrate temperature	450 °C,
source temperature	550 °C,
Te compensation temperature	220 °C,
growth rate	4.9 μm/h.

The carrier concentration n and mobility μ were determined between 14 and 300 K from the Hall voltage and resistivity using the van der Pauw method (Fig. 5). Since the curves flatten out at the lower temperatures, the 14 K values $\mu = 5.15 \times 10^5$ cm²/Vs and $n = 6.36 \times 10^{16}$ cm^{-3} may be used as material parameters for 4.2 K.

Discussion

In order to compare our data with those of previous publications, we have analyzed the dielectric constant with the sum of the lattice-oscillator and Drude terms:

$$\varepsilon(\tilde{\nu}) = \varepsilon_\infty + \frac{(\varepsilon_0 - \varepsilon_\infty)\tilde{\nu}_{TO}^2}{\tilde{\nu}_{TO}^2 - \tilde{\nu}^2 - i\tilde{\nu}\gamma} - \frac{\tilde{\nu}_p^2 \varepsilon_\infty}{\tilde{\nu}^2 + i\tilde{\nu}\Gamma}. \quad (1)$$

ε_0 and ε_∞ are the static and optical dielectric constants. The phonons are described by $\tilde{\nu}_{TO}$ and γ (the wavenumber of the transverse optical phonon and the damping factor in cm^{-1}). The plasma frequency is characterized by its wavenumber given by the equation:

$$\tilde{\nu}_p = \frac{1}{2\pi c}\sqrt{ne^2/\varepsilon_v \varepsilon_\infty m^*},$$

where e is the charge of an electron, ε_v the permittivity of vacuum and m^* the effective mass. We are justified in using a frequency independent electron damping Γ in the frequency range of interest, according to [11]. Using data from the literature, we anticipated finding measurable surface waves around $\tilde{\nu} = 100$ cm^{-1}.

Figure 6 shows our experimental values together with the theoretical value of ε as computed from (1). The theoretical curves were obtained using the maximum and minimum values of the parameters found in the literature. The electron damping factor Γ was chosen in order to keep the experimental data of the imaginary part of the dielectric constant consistent with the

Table 3

Parameter x	$F=\frac{\partial\varepsilon_r}{\partial x}\cdot\frac{x}{\varepsilon_r}$	$F=\frac{\partial\varepsilon_i}{\partial x}\cdot\frac{x}{\varepsilon_i}$
$\varepsilon_0=1267\pm50$	1.4	0.25
$\varepsilon_\infty=33$	−0.46	0.74
$\tilde{\nu}_{TO}=17.5\pm0.5\,cm^{-1}$	2.7	0.54
$\Gamma=4.5\,cm^{-1}$	$-5.3\cdot10^{-3}$	0.75
$\gamma=0.6\pm0.4\,cm^{-1}$	$2.5\cdot10^{-4}$	0.25
$\tilde{\nu}_p=72\pm5.5\,cm^{-1}$	1.2	−1.5

range of the theoretical values. This Γ is much higher than those given in the literature, but it should be considered with caution since it depends on the choice of other parameters. The discussion of the real part of ε will show that these parameters from the literature do not describe our sample well.

The experimental real part of ε turns out to be definitely higher than expected. Trying to find the origin of this discrepancy, we have calculated the influence of the above mentioned parameters on ε. This is given as a linear approximation by the equation $F=(\partial\varepsilon_{i,r}/\partial x)\cdot(x/\varepsilon_{i,r})$, for each parameter x and both the real and imaginary parts of ε. With this definition of F, the relative variation of ε due to a relative change $\Delta x/x$ in x is given by $F\cdot\Delta x/x$. For instance, a 1% rise in ε_0 will lower ε_r by 1.4%. The results are shown in Table 3, together with parameters for comparable samples, taken from the literature [4–6]. The uncertainties were either given in the literature or were determined from the range of values in the literature. The error in $\tilde{\nu}_p$ arises mainly from the error in the effective mass: $m^*=0.034\pm0.005\,m_0$ [12].

It is obvious that the decision to use a value of Γ fitted to our experiment cannot explain the differences in the real part of ε, as Γ hardly influences ε_r. In order to establish agreement with our experimental data, at least one of the parameters ε_0, $\tilde{\nu}_p$, or $\tilde{\nu}_{TO}$ that have a large influence on ε_r should have values smaller than those in the table, and/or ε_∞ should be larger. For example, if $\tilde{\nu}_{TO}=16.5\,cm^{-1}$ then the curve describing the upper limit intersects the error bars. Recent microwave experiments with similar samples yielded higher dielectric constants than those given in the previous literature [13]. This excludes the possibility of using a lower value for ε_0. Therefore one or more of the then remaining parameters is in error.

Conclusions

In principle, the six experimental values should be sufficient to calculate up to six independent parameters. In a prior, similar experiment at room temperature [8], we achieved errors of 3% to 10%. Errors of this order of magnitude allow a more exact determination of the parameters than was possible in this experiment. We hope to reduce the erros at cryogenic temperatures in the future to such levels.

Although surface polariton spectroscopy can only yield data for a limited number of frequencies, it will be of use in establishing or corraborating oscillator fits to other spectroscopic data. Our experimental data for the dielectric constant when compared to values computed from parameter values given in the literature for samples grown under comparable conditions, show that these parameter values do not hold for our sample.

An obvious advantage of these measurements is that thick layers or even bulk material may be used. This is in contrast to transmission experiments with high absorption and reflection. It is known, that PbTe samples should be quite thick in order to get "bulk" values for the epitaxial layers [5]. However, interference fringes which allow a good determination of the optical constants may be favourably used only up to a thickness of about 15 μm.

Acknowledgements. This work was supported in part by the „Deutsche Forschungsgemeinschaft". Calculations have been performed on the TR 440 of the Rechenzentrum, Universität Würzburg.

References

1. A. Otto: "Spectroscopy of surface polaritons by attenuated total reflection". In: *Optical Properties of Solids, New Developments*, ed. by B.D. Seraphin, (North Holland. Amsterdam 1976)
2. M.A. Kinch, D.D. Buss: Solid State Commun. **11**, 319 (1972)
3. H. Burkhard, G. Bauer, P. Grosse, A. Lopez-Otero: Phys. Stat. Sol. (b) **76**, 259 (1976)
4. H. Burkhard, G. Bauer, A. Lopez-Otero: Solid State Commun. **18**, 773 (1976)
5. H. Burkhard, G. Bauer, A. Lopez-Otero: J. Opt. Soc. Am. **67**, 943 (1977)
6. K. Shimizu, Y. Nisida, S. Narita: J. Phys. Soc. Jpn **46**, 1797 (1979)
7. M. von Ortenberg: "Submillimeter Magneto Spectroscopy of Charge Carriers by Use of the Strip-Line Technique". In: *Infrared and Millimeter Waves*, vol. 3, ed. by K.J. Button (Academic Press, New York 1980)
8. W. Schuberth, M. Tacke: Int. J. IR and mm Waves **2**, 665 (1981)
9. C.J. Grebenkemper, J.P. Hagen: Phys. Rev. **80**, 89 (1950)
10. M.H. Edwards: Can. J. Phys. **36**, 884 (1958)
11. H. Burkhard, G. Bauer, A. Lopez-Otero: Phys. Rev. B **18**, 2935 (1978)
12. R. Dalven: Infrared Phys. **9**, 141 (1969)
13. H. Lehmann, G. Nimtz, L.D. Haas: Verhandl. DPG (VI) **16**, 221 (1981)
14. H. Wolter: In: *Handbuch der Physik*, vol. XXIV, ed. by S. Flügge, (Springer, Berlin, Göttingen, Heidelberg 1956)